Discovery of BI 224436, a Noncatalytic Site Integrase Inhibitor (NCINI) of HIV-1

Lee D. Fader,*,[†] Eric Malenfant, Mathieu Parisien, Rebekah Carson, François Bilodeau, Serge Landry, Marc Pesant, Christian Brochu, Sébastien Morin, Catherine Chabot, Ted Halmos, Yves Bousquet, Murray D. Bailey, Stephen H. Kawai,[‡] René Coulombe, Steven LaPlante, Araz Jakalian, Punit K. Bhardwaj,[#] Dominik Wernic,[○] Patricia Schroeder,[⊥] Ma'an Amad, Paul Edwards, Michel Garneau, Jianmin Duan, Michael Cordingley, Richard Bethell, Stephen W. Mason,[§] Michael Bös, Pierre Bonneau, Marc-André Poupart, Anne-Marie Faucher, Bruno Simoneau, Craig Fenwick, Christiane Yoakim, and Youla Tsantrizos[‖]

Research and Development, Boehringer Ingelheim (Canada) Ltd., 2100 Cunard Street, Laval, Québec H7S 2G5, Canada

S *Supporting Information*

ABSTRACT: An assay recapitulating the 3′ processing activity of HIV-1 integrase (IN) was used to screen the Boehringer Ingelheim compound collection. Hit-to-lead and lead optimization beginning with compound **1** established the importance of the C3 and C4 substituent to antiviral potency against viruses with different aa124/aa125 variants of IN. The importance of the C7 position on the serum shifted potency was established. Introduction of a quinoline substituent at the C4 position provided a balance of potency and metabolic stability. Combination of these findings ultimately led to the discovery of compound **26** (BI 224436), the first NCINI to advance into a phase Ia clinical trial.

HTS hit
1

EC_{50} = >40,000 nM

BI 224436
26

EC_{50} = 11–27 nM

KEYWORDS: HIV Integrase, allosteric inhibitor, LTR DNA 3′-processing, NCINI
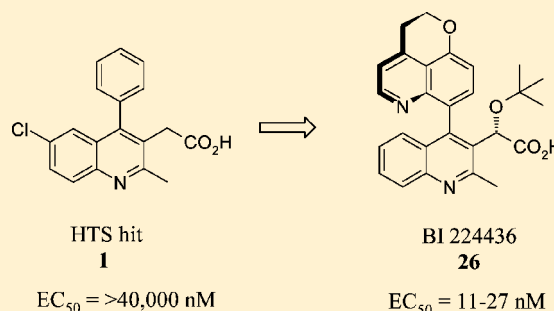
Since the discovery of the human immunodeficiency virus (HIV) in 1983, 25 million people have died from HIV-related disease.[1] Combination antiretroviral therapy (cART) was introduced in the mid-1990s and has led to a marked reduction of mortality and morbidity in HIV infected individuals.[2] For decades the drugs available for treatment of HIV were targeted to the essential viral enzymes reverse transcriptase (RT) and HIV protease. However, development of cross-resistance within mechanistic classes and poor tolerability necessitated the search for new targets for therapeutic intervention.[3−5] After considerable efforts from numerous academic and industrial laboratories, a third enzyme required for viral replication, integrase (IN), emerged as a viable target for HIV therapy. IN is responsible for the integration of viral DNA into host cell genome via a two-step process.[6,7] In the first step, IN binds to viral DNA as part of the preintegration complex (PIC) in the cytoplasm and excises a dinucleotide from each 3′-end. Following this 3′-processing event, the PIC is transported into the nucleus where the 3′-ends of viral DNA are covalently linked to the 5′-ends of the host cell DNA in a process known as strand transfer. An intense effort dedicated to the discovery and development of strand transfer inhibitors has led to approval of raltegravir, elvitegravir, and dolutegravir, which have changed the landscape of treatment options available to individuals living with HIV.[8−10]

However, there are no approved agents that target alternative functions of IN.

As part of our HIV drug discovery efforts, we initiated an HTS campaign toward identification of inhibitors of IN-catalyzed 3′-processing. We designed an assay that recapitulates the 3′-processing activity of IN in isolation from the strand transfer event using an LTR-like DNA substrate modified with a 5′-fluorophore/3′-fluorescence quencher pair. Upon action of IN, the fluorescence quencher covalently linked to the excised dinucleotide is liberated from the DNA duplex and fluorescence is restored. This assay was used to screen the Boehringer Ingelheim compound collection, which resulted in the identification of a hit series exemplified by compound **1**.[11] Isothermal calorimetry and equilibrium dialysis experiments confirmed that this series of compounds bound to IN with a binding stoichiometry of one molecule of inhibitor for every two molecules of the catalytic core domain (CCD) of IN. Building on the work of Dyda et al.,[12] we performed X-ray crystallographic experiments that demonstrated that this series of compounds bound to a hydrophobic pocket at the dimer interface of the CCD of IN (vide infra). This pocket was first
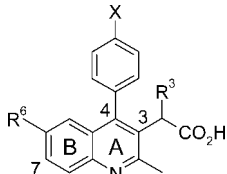
identified as the binding site of tetraarylarsonium ions by X-ray crystallography[13] and later as a part of the recognition domain on IN for the lens epithelial derived growth factor (LEDGF/p75),[14] a host cell protein involved in protection and trafficking of PICs to transcriptionally active regions of chromatin.[15] Since our series of inhibitors bound to a site remote from the active site and inhibited the 3′-processing activity of the enzyme, we have termed these molecules noncatalytic site integrase inhibitors (NCINIs). Herein we describe our optimization of HTS hit compound **1** and identification of BI 224436, the first clinical candidate from this mechanistic class of inhibitors.[16]

Compound **1** can be divided into three strategic substructures for modification: the C3 acetic acid moiety, the C4 arene, and the B-ring. Accordingly, we devised three distinct retrosynthetic disconnections, each designed to introduce these substructures late in the synthetic sequence (Figures S1–S3, Supporting Information). As part of our hit-to-lead activities, analogues of compound **1** were prepared in order to establish structure−activity relationships (SAR) and the minimal structural features required for inhibition of 3′-processing. We found that the chloro-substituent at C6 could be exchanged for another halogen, for example, giving bromo analogue **2** that was nearly equipotent in the LTR cleavage assay (Table 1).

Table 1. Preliminary SAR of X, R^6, and R^3 Substituents

	R^3	R^6	X	$K_{d\text{-app}}^a$ (μM)	IC_{50}^b (μM)	EC_{50}^c (μM)	CC_{50}^d (μM)
1	H	Cl	H		9.1	>40	
2	H	Br	H		5.1	>33	
3	H	H	H		24		
4	H	Br	Me		0.35	20	
5	H	Br	Cl		0.27	16	>64
6	H	H	Cl		3.1	>43	
7	Me	Br	Cl		0.31	13	
8	n-Pr	Br	Cl		0.077	0.92	94
9	OMe	Br	Cl		0.040	0.99	>64
10	(R)-OMe	Br	Cl		3.1	47	
11	(S)-OMe	Br	Cl	4.7	0.028	0.45	>51
12	(S)-Oi-Pr	Br	Cl	0.28		0.13	>50
13	(S)-Ot-Bu	Br	Cl	0.15		0.078	>5

$^a K_{d\text{-app}}$ determined using displacement assay. $^b IC_{50}$ determined with LTR-cleavage assay. $^c EC_{50}$ determined with HxB2 virus (A124/T125 IN variant). $^d CC_{50}$ determined as previously described (see ref 18).

However, when the halogen was removed, the compound was 3- to 5-fold less potent (cf., compound **3** to **1** and **2**). Exploration of substitution on the C4 phenyl ring revealed that addition of a 4-Me (**4**) or 4-Cl (**5**) substituent led to potency improvements of greater than 10-fold in the LTR cleavage assay. This improvement in intrinsic potency also brought about measurable antiviral potency in a viral replication assay.[17] As expected, removal of the bromo substituent from compound **5** led to a decrease in potency for analogue **6**. Taken together, the results demonstrated preliminary SAR and highlighted contributions from both the B-ring and C4 aryl group to potency.

Having established the importance of B-ring and C4-aryl substitutions, we selected compound **5** as a starting point for further optimization. A key finding was that growing from the α-position of the C3-acetic acid moiety generally improved potency. While the methyl substituted analogue **7** was equipotent to compound **5**, increasing the size of the alkyl substituent led to an improvement in intrinsic and antiviral activity. A leading example of this is the propyl analogue **8**, which showed IC_{50} value below 100 nM, an EC_{50} value below 1 μM for the first time, and a cytotoxicity window of >66-fold.[18] On the basis of these encouraging results, we explored a number of substituents at the α-position and discovered that further improvements in potency could be realized with alkoxyl groups. The simple methoxyl analogue **9** showed comparable activity to compound **8** and was separated into individual enantiomers for evaluation of a possible eutomer effect. The R-stereoisomer **10** exhibited reduced intrinsic and antiviral potency (>75- and >45-fold, respectively), while the S-enantiomer **11** was approximately 2-fold more active in both assays.

Compound **11** and closely related analogues have been used by us[16] and others[19,20] to study the bioactive conformation of our series of inhibitors by X-ray crystallography. As shown in Figure 1, the C3 substituent is critical to the binding of
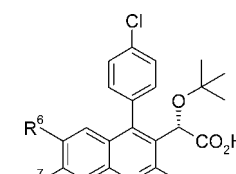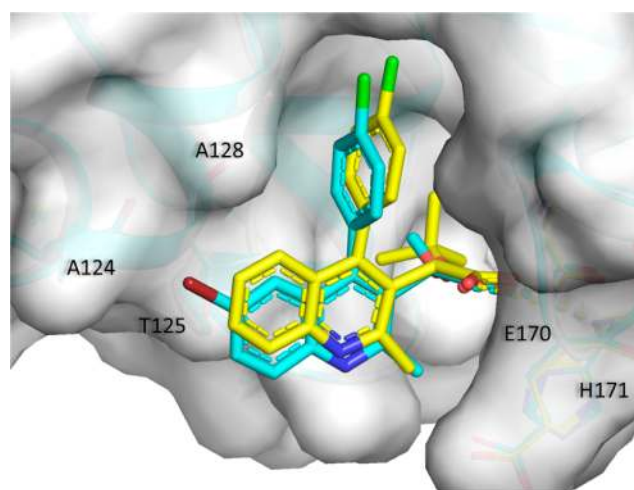

Figure 1. Ribbon representation of the superposition of compounds **11** and **16** bound to the CCD of IN, including a semitransparent surface of the CCD (PDB accession code 4NYF). The tube representations of **11** and **16** are colored by atom type, where cyan = carbon for **11**, yellow = carbon for **16**, blue = nitrogen, red = oxygen, green = chlorine, and maroon = bromine.

compound **11** to the CCD of IN and makes two key contacts with the protein: (a) a bivalent hydrogen bonding interaction with protein backbone at residues E170 and H171, and (b) a van der Waals contact deep in the hydrophobic pocket via the methoxyl group. The quinoline scaffold lies flat on the surface of the protein partially covering residues 124 and 125 and makes productive contact with the methyl group of A128. The plane of the C4-aryl group is orthogonal to that of the quinoline scaffold and also occupies space within the same deep hydrophobic pocket as the methoxyl substituent. Within group M isolates of HIV-1, residues 124 and 125 are polymorphic. With this in mind, a central theme to our potency optimization effort was to improve binding contacts made to the highly conserved regions of the pocket through an initial focus on the

C3 substituent. For this, we developed a displacement assay to measure apparent dissociation constants.[21] In this assay, compound **11** had a $K_{d\text{-app}}$ value of 4.7 μM. As we increased the size of the alkoxyl substituent on the C3 substituent in order to continue to fill the deep, hydrophobic pocket, we saw increases in binding affinity that correlated with increases in antiviral potency. After a survey of alkoxyl analogues, the -O*t*-Bu group emerged as the optimal substituent at this position (exemplified by analogue **13**, EC$_{50}$ = 78 nM).

Having optimized the R^3 substituent for binding to IN, we returned our focus to B-ring substitution patterns. Using compound **13** as a starting point, we conducted multiple positional scans and found that the most productive SAR came from substitutions at the R^6 and R^7 positions (Table 2). This

Chart 1. Evolution of the C4-Arene

Table 2. B-Ring SAR

	R^6	R^7	$K_{d\text{-app}}$ (nM)^a	EC$_{50}$ A124/T125 (nM)^b	EC$_{50}$ T124/A125 (nM)^c	CC$_{50}$ (μM)
13	Br	H	150	78	610	>5
14	F	H	61	28	70	
15	Me	H	48	27	160	48
16	H	H	49	23	110	86
17	H	F	68	26	91	>22
18	H	Cl	140	31	120	
19	H	Me	40	13	130	>86

^{a}Determined using displacement assay. ^{b}Determined with HxB2 virus (A124/T125 IN variant). ^{c}Determined with recombinant NL4.3 virus (T125A IN mutant).

Table 3. Optimization of Potency and Metabolic Stability

	R^4	EC$_{50}$ A124/T125 (nM)^a	EC$_{50}$ T124/A125 (nM)^b	HLM $t_{1/2}$ (min)	serum shift^c
19	A	13	130	230	25
20	B	7	22	24	66
21	C	2	22		83
22	D		29	65	15
23	E	34	300	>300	4.0
24	F	6	21	210	4.7

^{a}Determined with HxB2 virus (A124/T125 IN variant). ^{b}Determined with recombinant NL4.3 virus (T125A IN mutant). ^{c}Determined by measurement of EC$_{50}$ values ±50% human serum.

was especially true when we took into account a number of different *aa*124/*aa*125 variants. For example, the EC$_{50}$ value for the T124/A125 variant for compound **13** was 8-fold higher than the A124/T125 variant. Scanning the C6 position revealed that this gap could be minimized (cf., compound **13** to **14** and **15**). Interestingly, the antiviral potency for the unsubstituted analogue **16** was similar to compounds **14** and **15**. When this exercise was carried out at the C7 position, a comparable level of potency was obtained. However, a matched pair analysis revealed that the antiviral potency across a number of IN variants was consistently superior (2- to 3-fold) for the case of a methyl group compared to hydrogen at the C7 position. On the basis of this finding, we regularly incorporated this modification throughout lead optimization. Interestingly, X-ray cocrystallography revealed that removal of the C6–Br atom resulted in a shift of the quinoline scaffold to bring the C5 position in closer proximity to A128 and the C4 substituent deeper into the highly conserved region of the pocket, as exemplified by a comparison of compounds **11** and **16** (Figure 1).

In parallel with optimization of antiviral potency, we routinely characterized our inhibitors in a standard battery of in vitro ADME assays. The profiles of representative compounds selected from Table 3 are presented in Table S1, Supporting Information, and highlight excellent solubility and Caco-2 permeability, insignificant inhibition of the cytochrome P450 isozymes 3A4 and 2D6, and reasonable metabolic stability
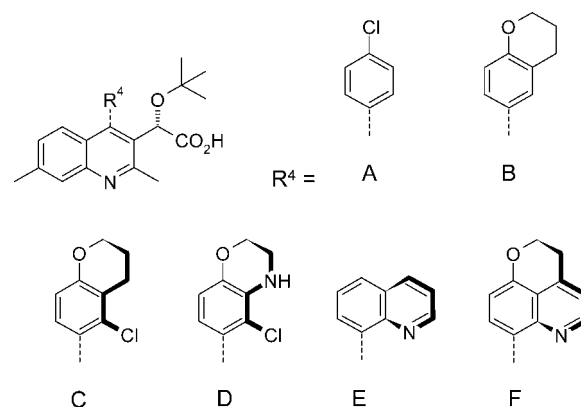
when incubated with either human or rat liver microsomes. Indeed, further improvement in antiviral potency was the key challenge we faced at this stage of the project.

An in-depth exploration of the C4 substituent proved to be the most productive path toward increases in antiviral potency. Our approach centered on optimal space-filling of the highly conserved regions of the binding pocket through desymmetrization of the C4 arene. Chart 1 tracks the evolution of the C4 arene with representative compounds within the C7-methyl series. A guiding design principle centered on linking the X and Y groups in structure **S12** (Scheme S2, Supporting Information) to give bicyclic C4 arenes, exemplified by the chromane analogue **20**, which led to improvements in antiviral potency (Table 3). Additionally, we noticed that the fold shift between EC$_{50}$ values measured with virus having different *aa*124/*aa*125 variants of IN decreased as we continued to fill the highly conserved portion of the pocket. Another key observation was that introducing substituents that restricted rotation about the C4−C(arene) bond often improved antiviral potency further. A leading example of this is when chloro analogue **21** is isolated as a stable atropisomer. Unfortunately, the saturated ring of the C4 arene introduced a site that was highly susceptible to metabolic oxidation in liver microsomal preparations. We found that introduction of polarity into the saturated ring, as with morpholine analogue **22** could only partially address this problem. In parallel with the exploration of motifs such as the C4-chromane, we also discovered the quinoline modification exemplified by compound **23**. Initially, we struggled to balance potency and the shift between IN variants in this series, but noted that the metabolic stability was generally excellent. The key breakthrough for our program came when we hybridized the chromane and quinoline systems to give the tricyclic C4 arenes exemplified by compound **24**.

This molecule regained potency across integrase variants and exhibited excellent metabolic stability.

While the optimization strategy for antiviral potency in Table 3 was successful in identifying the lead compound 24, we also noted a profound effect on EC_{50} value when the antiviral assays were performed in the presence of human serum (Table 3). The serum shifted (ss) EC_{50} has been used in human dose predictions for HIV preclinical candidate selection and therefore became a critical optimization parameter.[22] A series of retrospective analyses uncovered structural features that strongly impacted the serum shift value. The critical finding is highlighted in Figure 2, which compares all serum shift data
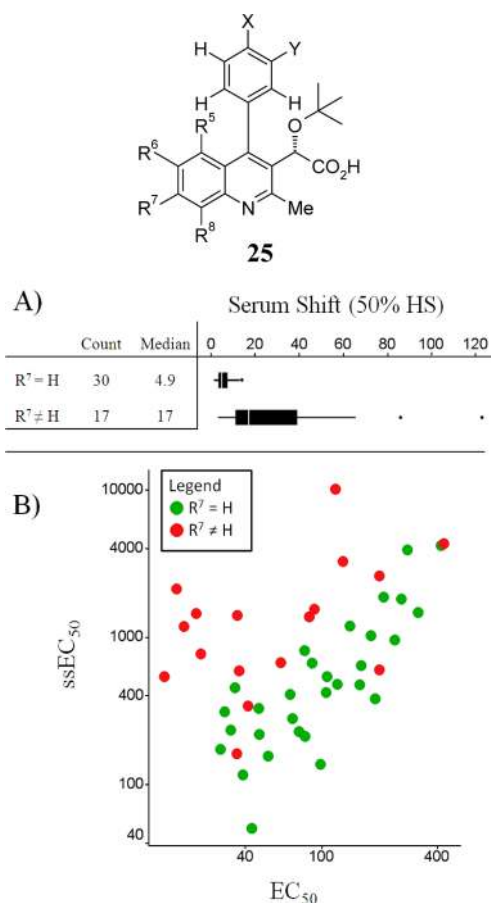

Figure 2. Effect of C7 substitution on serum shift for compounds with substructure 25. (A) Box plot (N = 47 compounds) showing difference in serum shift for compounds with or without R7 substituents. (B) Scatter plot of $ssEC_{50}$ vs EC_{50} (nM) for the same 47 compounds). Determined using recombinant NL4.3 virus (T124A IN mutant).

available for compounds having substructure 25. When the data is binned according to the R^7 substituent, we see that compounds where R^7 = H have significantly lower serum shift values than those with any other substituent at this position (Figure 2A). Furthermore, a scatter plot of $ssEC_{50}$ vs EC_{50} highlights that at all levels of antiviral potency, the negative impact of serum shift on potency is generally greater for C7 substituted compounds (Figure 2B). On the basis of this analysis, removal of the C7-methyl group from 24 led us to compound 26 (BI 224436), a compound with antiviral potency slightly better than expected based on the results presented in Table 3, but with improved serum shift, excellent metabolic

stability and the generally favorable in vitro ADME profile characteristic of this series (Table 4). Compound 26 was also

Table 4. In Vitro ADME Profile of Compound 26

BI 224436
26
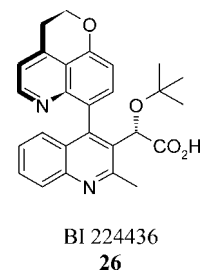
EC_{50} range,[a] nM	11−27
serum shift (50% HS), fold-change[b]	2.1
HLM/RLM ($t_{1/2}$), min	210/>300
Caco-2 (P_{app}), × 10^6 cm/s	14
CyP450 inh. (IC_{50}, 3A4/2D6), μM	23/>30
$logD_{7.4}$	0.44
solubility[c] (pH = 6.8), mg/mL	>0.85

[a]Determined with HxB2 virus (A124/T125 IN variant), NL4.3 virus (T124/T125), or recombinant NL4.3 virus (A124/T125, A124/A125, N124/T125, or N124/A125 IN variants) as previously described. [b]Determined by measurement of EC_{50} values ±50% human serum. [c]For the amorphous powder.

evaluated in a rat pharmacokinetic experiment (0.2 mg/kg i.v.; 0.4 mg/kg p.o.) and exhibited an excellent half-life (8.8 h) and good oral bioavailability (F = 54%). On the basis of these findings, compound 26 was advanced into further preclinical profiling, the complete results of which will be reported elsewhere.

In conclusion, we have used an assay based on the 3′ processing activity of HIV-1 IN to screen the Boehringer Ingelheim compound collection and identify hit compound 1.[23−29] Hit-to-lead and lead optimization effort established the importance of the C3 and C4 substituents to binding to the CCD of IN, which translated into excellent antiviral potency against a number of viruses with different $aa124/aa125$ variants of IN. We also established the importance of the C7 position on the serum shifted potency. Balancing good potency with excellent metabolic stability was achieved through the introduction of a quinoline substituent at the C4 position. Combination of these findings ultimately led to the discovery of compound 26 (BI 224436), the first NCINI to advance into a phase Ia clinical trial.

■ ASSOCIATED CONTENT

Ⓢ Supporting Information

Synthetic schemes for preparation of NCINIs and characterization of key compounds. This material is available free of charge via the Internet at http://pubs.acs.org.

■ AUTHOR INFORMATION

Corresponding Author

*(L.D.F.) E-mail: lee.fader@boehringer-ingelheim.com. Phone: +1 (203) 791-6766.

Present Addresses

†Boehringer Ingelheim Pharmaceuticals, Inc., 900 Ridgebury Road, Ridgefield, Connecticut 06877, United States.

‡Department of Chemistry and Biochemistry, Concordia University, 7141 Sherbrooke Street West, Montreal, QC H4B 1R6, Canada.

§Bristol-Myers Squibb, Virology, 5 Research Parkway, Wallingford, Connecticut 06492, United States.

∥Department of Chemistry, McGill University, 801 Sherbrooke Street West, Montreal, QC H3A 0B8, Canada.

⊥EMD Serono, 45 Middlesex Turnpike, Billerica, Massachusetts 01821, United States.

#Toronto Research Chemicals, 2 Brisband Road, North York, ON M3J 2J8, Canada.

○Lady Davis Institute, Jewish General Hospital, 3755 Côte Ste-Catherine Road, Montreal, QC H3T 1E2, Canada.

Notes

The authors declare no competing financial interest.

■ ABBREVIATIONS

cART, combination antiretroviral therapy; HTS, high-throughput screen; LTR, long terminal repeat; HLM, human liver microsomes; RLM, rat liver microsomes

■ REFERENCES

(1) World Health Organization. Factsheet No. 360, updated June 30, 2013. http://www.who.int/mediacentre/factsheets/fs360/en/index.html (accessed July 14, 2013).

(2) Palella, F. J., Jr.; Delaney, K. M.; Moorman, A. C.; Loveless, M. O.; Fuhrer, J.; Satten, G. A.; Aschman, D. J.; Holmberg, S. D. Declining morbidity and mortality among patients with advanced human immunodeficiency virus infection. *N. Engl. J. Med.* **1998**, *338*, 853−860.

(3) Carr, A.; Cooper, D. A. Adverse effects of antiretroviral therapy. *Lancet* **2000**, *356*, 1423−1430.

(4) Reisler, R. B.; Han, C.; Burman, W. J.; Tedaldi, E. M.; Neaton, J. D. Grade 4 events are as important as AIDS events in the era of HAART. *J. Acquired Immune Defic. Syndr.* **2003**, *34*, 379−386.

(5) Clavel, F.; Hance, A. J. HIV drug resistance. *N. Engl. J. Med.* **2004**, *350*, 1023−1035.

(6) Craigie, R. The molecular biology of HIV integrase. *Future Virol.* **2012**, *7*, 679−686.

(7) McColl, D. J.; Chen, X. Strand transfer inhibitors of HIV-1 integrase: bringing IN a new era of antiretroviral therapy. *Anti-Viral Res.* **2010**, *85*, 101−118.

(8) Raffi, F.; Wainberg, M. A. Multiple choices for HIV therapy with integrase strand transfer inhibitors. *Retrovirology* **2012**, *9*, 110.

(9) Arribas, J. R.; Eron, J. Advances in antiretroviral therapy. *Curr. Opin. HIV AIDS* **2013**, *8*, 341−349.

(10) Calin, R.; Katlama, C. The place of raltegravir in the clinical management of HIV-1 infection. *Clin. Pract.* **2013**, *10*, 427−438.

(11) For the first disclosure of the synthesis and biological activity of this series of inhibitors see: Tsantrizos, Y. S.; Boes, M.; Brochu, C.; Fenwick, C.; Malenfant, E.; Mason, S.; Pesant, M. Inhibitors of Human Immunodeficiency Virus Replication PCT Int. Appl. WO 2007/131350.

(12) Dyda, F.; Hickman, A. B.; Jenkins, T. M.; Engelman, A.; Craigie, R.; Davies, D. R. Crystal structure of the catalytic domain of HIV-1 integrase: similarity to other polynucleotidyl transferases. *Science* **1994**, *266*, 1981−1986.

(13) Molteni, V.; Greenwald, J.; Rhodes, D.; Hwang, Y.; Kwiatkowski, W.; Bushman, F. D.; Siegel, J. S.; Choe, S. Identification of a small-molecule binding site at the dimer interface of the HIV integrase catalytic domain. *Acta Crystallogr., Sect. D: Biol. Crystallogr.* **2001**, *57*, 536−544.

(14) Cherepanov, P.; Ambrosio, A. L.; Rahman, S.; Ellenberger, T.; Engelman, A. Structural basis for the recognition between HIV-1 integrase and transcriptional coactivator p75. *Proc. Natl. Acad. Sci. U.S.A.* **2005**, *102*, 17308−17313.

(15) Maertens, G.; Cherepanov, P.; Pluymers, W.; Busschots, K.; De Clercq, E.; Debyser, Z.; Engelborghs, Y. LEDGF/p75 Is essential for nuclear and chromosomal targeting of HIV-1 integrase in human cells. *J. Biol. Chem.* **2003**, *278*, 33528−33539.

(16) Parts of this work have been presented at the following conferences: (a) Fenwick, C.; Bethell, R.; Bonneau, P.; Duan, J.; Faucher, A.-M.; Mason, S.; Poupart, M.-A.; Simoneau, B.; Tsantrizos, Y.; Yoakim, C. Identification of BI-C, a novel HIV-1 non-catalytic site integrase inhibitor. *18th Conference on Retroviruses and Opportunistic Infections*, Boston, MA, USA, 27 February−3 March, 2011 (abstract 523). (b) Simoneau, B.; Amad, M.; Bailey, M. D.; Bethell, R.; Bhardwaj, P. K.; Bilodeau, F.; Bonneau, P.; Bös, M.; Bousquet, Y.; Brochu, C.; Carson, R.; Chabot, C.; Cordingley, M.; Coulombe, R.; Duan, J.; Edwards, P.; Fader, L.; Faucher, A.-M.; Fenwick, C.; Garneau, M.; Halmos, T.; Jakalian, A.; Kawai, S.; Landry, S.; Laplante, S.; Malenfant, E.; Mason, S.; Morin, S.; Parisien, M.; Pesant, M.; Poupart, M.-A.; Tsantrizos, Y.; Wernic, D.; Yoakim, C. Identification of Novel Non-Catalytic Site Integrase Inhibitors (NCINIs) of LTR DNA 3′ Processing. *24th International-Conference on Antiviral Research*, Sofia, Bulgaria, May 8−11th, 2011 (Late Breaker abstract).

(17) All EC_{50} values were determined luciferase reporter gene assay as previously described and are the average of at least two experiments. For cases where averages are for 3 or more experiments, relative standard deviations ranged from 12 to 43%. See refs 11 and 21.

(18) CC_{50} determinations were made as previously described: Rajotte, D.; Tremblay, S.; Pelletier, A.; Salois, P.; Bourgon, L.; Coulombe, R.; Mason, S.; Lamorte, L.; Sturino, C. F.; Bethell, R. Identification and characterization of a novel HIV-1 nucleotide-competing reverse transcriptase inhibitor series. *Antimicrob. Agents Chemother.* **2013**, *57*, 2712−2718.

(19) Christ, F.; Voet, A.; Marchand, A.; Nicolet, S.; Desimmie, B. A.; Marchand, D.; Bardiot, D.; Van der Veken, N. J.; Van Remoortel, B.; Strelkov, S. V.; De Maeyer, M.; Chaltin, P.; Debyser, Z. Rational design of small-molecule inhibitors of the LEDGF/p75-integrase interaction and HIV replication. *Nat. Chem. Biol.* **2010**, *6*, 442−448.

(20) Feng, L.; Sharma, A.; Slaughter, A.; Jena, N.; Koh, Y.; Shkriabai, N.; Larue, R. C.; Patel, P. A.; Mitsuya, H.; Kessl, J. J.; Engelman, A.; Fuchs, J. R.; Kvaratskhelia, M. The A128T resistance mutation reveals aberrant protein multimerization as the primary mechanism of action of allosteric HIV-1 integrase inhibitors. *J. Biol. Chem.* **2013**, *288*, 15813−15820.

(21) Bailey, M. D.; Bilodeau, F.; Carson, R. J.; Fader, L.; Halmos, T.; Kawai, S.; Landry, S.; Laplante, S.; Simoneau, B.; Tsantrizos, Y. S. Inhibitors of Human Immunodeficiency Virus Replication. PCT Int. Appl. WO 2009/062289

(22) Molla, A.; Vasavanonda, S.; Kumar, G.; Sham, H. L.; Johnson, M.; Grabowski, B.; Denissen, J. F.; Kohlbrenner, W.; Plattner, J. J.; Leonard, J. M.; Norbeck, D. W.; Kempf, D. J. Human serum attenuates the activity of protease inhibitors toward wild-type and mutant human immunodeficiency virus. *Virology* **1998**, *250*, 255−262.

(23) In spite of the fact that the NCINI class of HIV inhibitors was discovered using a 3′-processing assay, recent study of NCINI's has revealed that their primary antiviral effect takes place at the stage of particle assembly and viral maturation and not at the early stage of the viral replication cycle associated with the IN 3′ processing activity. See refs 24−29.

(24) Balakrishnan, M.; Yant, S. R.; Tsai, L.; O'Sullivan, C.; Bam, R. A.; Tsai, A.; Niedziela-Majka, A.; Stray, K. M.; Sakowicz, R.; Cihlar, T. Non-catalytic site HIV-1 integrase inhibitors disrupt core maturation and induce a reverse transcription block in target cells. *PLoS One* **2013**, *8*, e74163−e74163.

(25) Jurado, K. A.; Wang, H.; Slaughter, A.; Feng, L.; Kessl, J. J.; Koh, Y.; Wang, W.; Ballandras-Colas, A.; Patel, P. A.; Fuchs, J. R.; Kvaratskhelia, M.; Engelman, A. Allosteric integrase inhibitor potency is determined through the inhibition of HIV-1 particle maturation. *Proc. Natl. Acad. Sci. U.S.A.* **2013**, *110*, 8690−8695.

(26) Feng, L.; Sharma, A.; Slaughter, A.; Jena, N.; Koh, Y.; Shkriabai, N.; Larue, R. C.; Patel, P. A.; Mitsuya, H.; Kessl, J. J.; Engelman, A.; Fuchs, J. R.; Kvaratskhelia, M. The A128T resistance mutation reveals aberrant protein multimerization as the primary mechanism of action of allosteric HIV-1 integrase inhibitors. *J. Biol. Chem.* **2013**, *288*, 15813−15820.

(27) Christ, F.; Shaw, S.; Demeulemeester, J.; Desimmie, B. A.; Marchand, A.; Butler, S.; Smets, W.; Chaltin, P.; Westby, M.; Debyser, Z.; Pickford, C. Small-molecule inhibitors of the LEDGF/p75 binding site of integrase block HIV replication and modulate integrase multimerization. *Antimicrob. Agents Chemother.* **2012**, *56*, 4365−4374.

(28) Tsiang, M.; Jones, G. S.; Niedziela-Majka, A.; Kan, E.; Lansdon, E. B.; Huang, W.; Hung, M.; Samuel, D.; Novikov, N.; Xu, Y.; Mitchell, M.; Guo, H.; Babaoglu, K.; Liu, X.; Geleziunas, R.; Sakowicz, R. New class of HIV-1 integrase (IN) inhibitors with a dual mode of action. *J. Biol. Chem.* **2012**, *287*, 21189−21203.

(29) Kessl, J. J.; Jena, N.; Koh, Y.; Taskent-Sezgin, H.; Slaughter, A.; Feng, L.; de Silva, S.; Wu, L.; Le Grice, S. F. J.; Engelman, A.; Fuchs, J. R.; Kvaratskhelia, M. Multimode, cooperative mechanism of action of allosteric HIV-1 integrase inhibitors. *J. Biol. Chem.* **2012**, *287*, 16801−16811.